

Mobilization of Reinforcement Tension within Geosynthetic-Reinforced Soil Structures

Kuo-Hsin Yang¹, Jorge G. Zornberg² and Richard J. Bathurst³

1. Assistant Professor, Construction Engineering Dept., National Taiwan University of Science and Technology; E-mail: khy@mail.ntust.edu.tw
2. Associate Professor, Civil, Environmental and Architectural and Environmental Engineering Dept., The University of Texas at Austin, E-mail: zornberg@mail.utexas.edu
3. Professor, Civil Engineering Dept., Royal Military College of Canada, E-mail: bathurst-1@rmc.ca

ABSTRACT

This paper examines the mobilization of reinforcement tension within geosynthetic-reinforced soil (GRS) structures at working stress and at large soil strains. Fully-mobilized reinforcement tension is assumed in most current design methods for the internal stability of GRS structures. In these methods the mobilized reinforcement tensile load is assumed to be equal to mobilized horizontal soil forces computed using active earth pressure theory. However, comparison with reinforcement tension loads measured in the field has shown that this approach is conservative (excessively safe) by as much as a factor of two. This observation has prompted the current study in which stress data obtained from a numerical study and two instrumented large-scale GRS retaining walls were used to examine the relationship between mobilized reinforcement tensile load and mobilized soil shear strength. The results show that the ratio of reinforcement tensile load and mobilized soil shear strength is not constant. Only when the average mobilized soil shear strength exceeds 95%, is reinforcement tensile capacity mobilized significantly. Nevertheless, less than 30% of reinforcement strength is mobilized when the average mobilized soil shear strength reaches peak soil shear capacity. These results help explain why current design methods lead to computed reinforcement loads that are very high compared to measured loads under operational conditions.

Keywords: Reinforcement tension, GRS structure, Finite element analysis

INTRODUCTION

In FHWA design guidelines for Mechanically Stabilized Earth (MSE) retaining wall structures (Elias et al. 2001), earth pressure theory is used to predict reinforcement tensile loads for internal stability calculations. The design rationale assumes that the tensile loads developed in reinforcement layers are in local equilibrium with lateral earth pressures generated in MSE walls. The soil stress state within Geosynthetic-Reinforced Soil (GRS) structures along potential internal failure surfaces is assumed to be at active conditions due to the relative flexibility of geosynthetics which allows the surrounding soil to deform. Therefore, the internal stability design of GRS structures simply assumes that the mobilized reinforcement tensile load is equal to the soil horizontal forces developed at active conditions.

Christopher et al. (2005) reported that the maximum reinforcement loads estimated by using the lateral active earth pressure approach could over-predict actual loads by as much as a factor of two. Allen et al. (2003) and Bathurst et al. (2008, 2005) investigated quantitatively the accuracy of reinforcement loads predicted by earth pressure theory using careful interpretation of a database of 30 well-monitored full-scale walls. They also concluded that loads predicted using earth pressure theory were excessively conservative. The predicted loads for GRS walls were *on average* three times greater than estimated values for full-scale instrumented walls. To overcome these deficiencies, Allen et al. (2003) and Bathurst et al. (2008, 2005) proposed a new empirical-based working stress method for estimation of reinforcement loads in GRS walls (K-stiffness Method). However, the K-stiffness Method is empirical-based and thus does not provide insight into the actual physical mechanisms that lead to mobilization of soil shear strength and reinforcement load capacity. The objective of this paper is to examine the mobilization of reinforcement tensile loads within GRS structures at working stress conditions (operational conditions) and at large soil strains approaching an ultimate soil state. The results provide useful insight into mechanisms that lead to different rates and magnitude of mobilization of soil shear strength and reinforcement loads.

MODELING OF GRS SLOPE

Centrifuge Test

A series of centrifuge tests on GRS reinforced slopes was conducted by Arriaga (2003) to investigate the response of GRS slopes to various design factors, e.g. backfill relative density, slope angle, reinforcement vertical spacing and reinforcement type. One centrifuge test (slope M1), was selected for numerical simulation and verification.

The dimensions and reinforcement layout of slope M1 are illustrated in Figure 1. Monterey No. 30 sand with a target relative density of 70% was used as the backfill and foundation soil. For this relative density, the peak friction angle was 36.5° under triaxial compression conditions and 42.0° under plane strain conditions. The unit weight of the backfill was 16.0 kN/m^3 . The reinforcement used in the centrifuge study was a commercially available nonwoven geotextile. The average unconfined tensile strength from wide-width tensile tests was 0.03 kN/m . The confined tensile strength value, obtained from back-calculation at failure in the centrifuge slope models, was 0.124 kN/m (Arriaga 2003). Each slope model was loaded to failure and the g -level N_g required to fail the slope was recorded. Slope failure was determined by a sudden large increase in settlement measured by a LVDT at the front crest of the slope.

Finite Element Simulation

Finite element modeling was carried out using the in-house developed finite element program, Nonlinear Analysis of Geotechnical Program (ANLOG). ANLOG is coded in FORTRAN. The initial conditions for the slope M1 model are shown in Figure 1. An 8-node quadratic quadrilateral element under plane strain condition was used for the solid elements. Four gauss points were assigned to each solid element.

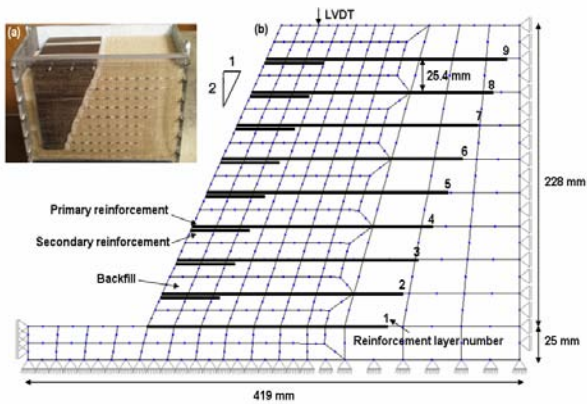


Figure 1. Slope M1 dimensions and layout

Standard boundary conditions were imposed to simulate confinement at the edges of aluminum centrifuge box. A small isotropic stress of 0.01 atm was applied to the first filled soil layer as initial stress field. Staged (layer by layer) construction was simulated. Mesh updating was used to account for large model deformations. The centrifugal force of the centrifuge was simulated by increasing the body force on each element. Each loading stage was applied in 5g increments. A total of 10 loading stages were applied. Hence, the final target g-level in the simulation was 50g.

The Lade-Kim elastoplastic constitutive model (Kim and Lade 1988; Lade and Jakobsen 2002; Lade and Kim 1995, 1988, and 1988b) and a proposed soil softening model (Yang 2009) were implemented in program ANLOG to model soil behavior at various stress states. As soil strength changes from hardening (pre-peak) to softening (post-peak), the yield surface changes from expansion to contraction. The yield surface contraction is governed by a soil softening model proposed by Yang (2009). The model captures the soil softening behavior using an inverse sigmoid function with the following features: 1) provides a smoother transition from hardening to softening after soil peak strength; 2) limits the decrease in size of the yield surface to a minimum (residual) yield surface during softening.

Reinforcement layers were simulated using bar elements with only one degree of freedom in the horizontal direction. A nonlinear elastic reinforcement model based on a second order polynomial was used to equate tensile load to tensile strain (Karpurapu and Bathurst 1995). The reinforcement model parameters were calibrated using the load-strain data from wide-width tensile tests.

Although the interaction and relative movement between reinforcement layers and backfill can be modeled using the interface element in the ANLOG program, the interface element was not applied in the numerical model to prevent numerical difficulty and to reduce computational cost. The approach used in the numerical modeling was supported by the visual observation that reinforcement specimens ruptured rather than failed due to pullout in the centrifuge tests. The readers are referred to Yang (2009) for more computational details of the finite element model simulation.

Model Verification

The simulation results were compared with centrifuge results to verify the accuracy of the proposed finite element model. Figure 2 shows that there is good qualitative agreement between physical and numerical deformation patterns at the moment of slope failure. In making comparisons the following observations are important: 1) sliding of the slope mass, 2) settlement at the top of the slope, and 3) failure surface above the slope toe. Both the centrifuge and numerical model showed a similar pattern of sliding of the slope mass and settlement at the location of the top LVDT. The settlement can be detected by comparing the original and deformed meshes at the slope top in the numerical model in Figure 2b. The failure surface in the vicinity of the toe was expected to pass through the toe based on conventional analysis. However, as shown in Figure 2a, the failure surface in slope M1 passed through the slope face at the second layer of reinforcement. This may be influenced by the boundary constraint due to the shallow thickness of foundation. This behavior was also captured in the numerical simulation as shown in Figure 2b.

The accuracy of the numerical model was also verified by quantitatively comparing the location of the failure surface, settlement at the slope crest with g-level and displacement along each reinforcement layer. In this regard, all predicted and measured results were judged by Yang (2009) to be in satisfactory agreement.

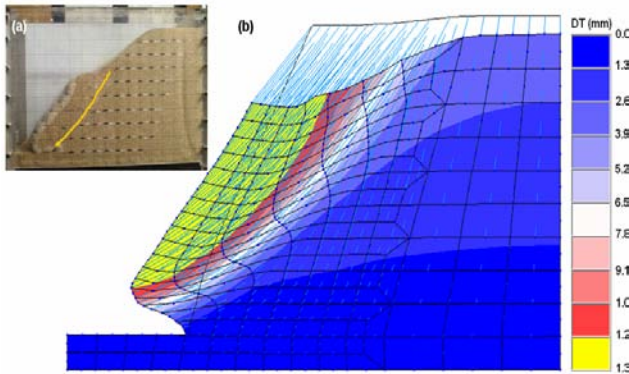


Figure 2. Comparison of deformation pattern: (a) Centrifuge model; (b) FE model (deformation x 20)

RESULTS FROM NUMERICAL SIMULATION

Definition of Strength Mobilization

The mobilization of soil shear strength can be quantified using soil stress level S defined in the Lade-Kim soil model as follows:

$$S = \frac{f_n}{\eta_1} \quad (1)$$

where f_n is the stress state on the current failure surface and η_1 is the corresponding failure criterion. One can also view the soil stress level S as an index of soil strength mobilization; i.e. the ratio of current mobilized soil shear strength to peak soil shear

strength. Figure 3 shows a typical simulation result of soil stress level contours and the corresponding stress states. The value of S is less than 1.0 when the current soil stress state is below the soil peak shear strength (Figure 3a). S equals 1.0 when the current soil stress state reaches the soil peak shear strength (Figure 3b).

When the current soil stress state exceeds the soil peak shear strength, the soil shear strength will decrease. This soil softening (post-peak) behavior can be modeled using the contraction of the yield surface in the soil softening model. As a result, the soil stress level S defined in Eq. (1) would be less than 1.0 during softening. In order to distinguish between soil stress levels during hardening and softening stages, it is necessary to define the soil stress level S during softening as follows:

$$S = 1 + \left(1 - \frac{f_n}{\eta_1}\right) \quad (2)$$

Here, the current soil stress state reaches the peak soil shear strength, $f_n = \eta_1$ and $S = 1.0$ in Eq. (2) and is consistent with Eq. (1) at peak shear strength mobilization. In the soil softening region, the range of S is from 1.0 to 2.0.

Similar to the definition for the mobilization of soil shear strength, the reinforcement stress level S_R is defined to quantify the mobilization of reinforcement tensile capacity as follows:

$$S_R = \frac{T_m}{T_{ult}} \quad (3)$$

where T_m is the mobilized peak reinforcement tension in each layer of reinforcement and T_{ult} is the ultimate tensile strength of the reinforcement.

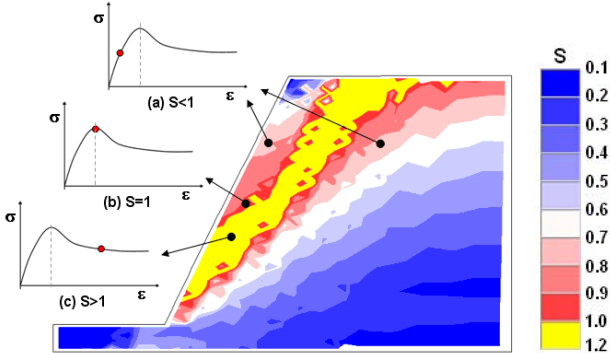


Figure 3. Soil stress level contours and illustration of corresponding stress states

Mobilization of Soil Shear Strength and Reinforcement Tension

The concurrent mobilization of reinforcement tensile load and soil strength is investigated in this section. Because soil shear strength and reinforcement loads along the failure surface are critical factors for the evaluation of system stability, the focus of this study is on the failure surface. The soil stress level S is obtained at the Gaussian point that is closest to the location of peak reinforcement load level S_R in each reinforcement layer. The results are presented in Figure 4. Relatively large variations in S (scatter in horizontal direction in Figure 4) are observed at low g -level

and relatively large variations of S_R (scatter in vertical direction in Figure 4) are observed at high g -level. This suggests that mobilization of soil shear strength is not uniform along the failure surface at low g -level (or at low S values) but becomes more uniform at high g -level (or at high S values when S approaches 1.0). In contrast, the mobilization of reinforcement tensile load at each layer is uniform at low g -level and becomes non-uniform at high g -level. Because of the scatter, average and upper bound values on reinforcement load level are provided. The average value of reinforcement load level is obtained by averaging all reinforcement layer loads. The upper bound value represents the mobilization of maximum peak reinforcement tensile load at each g -level increment.

In Figure 4, the most important observation is that the mobilization of reinforcement tensile load capacity does not increase linearly with the mobilization of soil shear strength; rather, there are two stages. In the first stage, the mobilization of reinforcement tensile load increases slowly to approximately 10% of its ultimate tensile strength until the average mobilized soil shear strength along the failure surface reaches about 95% of its peak shear strength. During the second stage, when the average mobilized soil shear strength exceeds 95%, reinforcement tensile load capacity is mobilized rapidly. Nevertheless, more than 30% of reinforcement strength is still available even when the average mobilized soil shear strength reaches the peak shear strength value ($S = 1$).

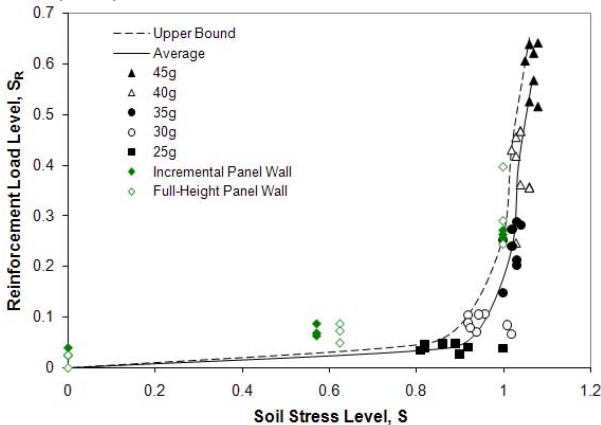


Figure 4: Comparison of the mobilization of reinforcement tensile load capacity and soil stress level (plus data from two full-scale instrumented walls)

RESULTS FROM TWO LARGE-SCALE TEST WALLS

Two instrumented large-scale GRS retaining walls 3m in height were tested to failure in the Royal Military College (RMC) retaining wall test facility (Bathurst 1993, Bathurst and Benjamin 1990, Bathurst et al. 1989, Karpurapu and Bathurst 1995). The GRS walls were constructed with a dense sand fill and layers of extensible geogrid reinforcement attached to two different facing treatments: incremental panel and full-height panel. Both walls were taken to collapse under uniform surcharge pressure applied to the top of the backfill. The strains developed at

each reinforcement layer were seen to increase as surcharge pressure was increased in steps. Reinforcement strains can be used to compute reinforcement tensile load in the physical tests using the load-extension response reported by Bathurst (1993). S_R can then be computed using the ultimate tensile strength of the reinforcement (reported as 12 kN/m) and S_R compared to numerical predicted values.

The soil failure mechanism in the large-scale GRS wall tests was detected during careful wall excavation by tracing a well-developed shear plane propagating through the reinforced soil zone commencing at the heel of the facing. Therefore, the average soil stress level S corresponding to this stage along this failure surface is assumed equal to 1.0 or slightly larger than 1.0. Because the soil stress levels along the failure surface before and after soil failure were not measured, the development of soil stress levels is assumed uniform along the failure surface and proportional to the magnitude of applied surcharge. Hence, S is taken as zero at end of construction before the application of surcharge and possible mobilization of soil shear strength during construction is neglected in this analysis.

Results obtained from the two instrumented walls are also plotted in Figure 4 and fall on the band of data obtained from numerical analysis of the centrifuge tests. The reinforcement load level S_R is generally higher than values obtained from numerical analysis of the centrifuge tests when $S < 1$. The difference may be due to compaction during wall construction which is not included in the numerical analysis.

DISCUSSION AND CONCLUSIONS

In this paper, stress data obtained from a numerical study of a centrifuge model slope and two physical full-scale instrumented GRS retaining walls were used to examine the relationship between mobilized reinforcement load capacity and mobilized soil shear strength. The results indicate that mobilization of reinforcement tensile load capacity does not increase linearly with mobilized soil shear strength up to soil failure. Rather reinforcement tensile load increases slowly to approximately 10% of its ultimate tensile strength until the average mobilized soil shear strength along the failure surface reaches about 95% of its peak shear. Even after the soil is at a post-peak shear strength state the reinforcement still retained an additional 30% of its original tensile load capacity.

The results obtained in this study help to explain the observation that measured reinforcement loads in geosynthetic reinforced soil walls under operational conditions are much less than predicted values using current force-equilibrium based design methods. This is because the soil shear strength within GRS structures is computed using classical active earth pressure theory and thus soil shear strength is assumed to be fully mobilized. However, based on the results shown in Figure 4, less than half of the reinforcement strength is mobilized at $S = 1$. Therefore, the over-prediction of maximum reinforcement loads by as much as a factor of two may be expected for walls at end of construction and under operational conditions.

In fact, soil and reinforcement strains and load are developed due to internal displacement of GRS structures. Hence, mobilized reinforcement tensile load in GRS structures are a function of the type of elongation and stiffness of the geosynthetic layers as they interact with and potentially influence and improve the confining soils. Consequently, design methodologies based on force equilibrium cannot be expected to predict accurate reinforcement loads. Rather, displacement-based analysis and

design methods hold promise as alternative approaches for the selection of reinforcement materials and for the internal stability analysis of GRS structures.

REFERENCES

- Allen, T.M., Bathurst, R.J., Holtz, R.D., Walters, D. and Lee, W.F. (2003) "A New Working Stress Method for Prediction of Reinforcement Loads in Geosynthetic Walls", *Canadian Geotechnical Journal*, v 40, n 5, p 976-994.
- Arriaga, F. (2003) "Response of Geosynthetic-Reinforced Structures under Working Stress and Failure Conditions", PhD Dissertation, Department of Civil Engineering, the University of Colorado, Boulder.
- Bathurst, R.J. (1993) "Investigation of Footing Restraint on Stability of Large-Scale Reinforced Soil Wall Tests", *46th Canadian Geotechnical Conference*, p 389-398.
- Bathurst, R.J., Allen, T.M. and Walters, D.L. (2005) "Reinforcement Loads in Geosynthetic Walls and the Case for a New Working Stress Design Method", *Geotextiles and Geomembranes*, v 23, n 4, p 287-322.
- Bathurst, R.J. and Benjamin, D.J. (1990) "Failure of a Geogrid Reinforced Soil Wall", *Transportation Research Record*, 1288, Washington, D.C., p 109-116.
- Bathurst, R.J., Benjamin, D.J. and Jarrett, P.M. (1989) "An Instrumented Geogrid Reinforced Soil Wall", *Proceedings of the Twelfth International Conference on Soil Mechanics and Foundation Engineering*, Rio de Janeiro, 13-18 August 1989.
- Bathurst, R.J., Miyata, Y., Nernheim, A. and Allen, T.M. (2008) "Refinement of K-Stiffness Method for Geosynthetic Reinforced Soil Walls", *Geosynthetics International*, v 15, n 4, p 269-295.
- Bathurst, R.J., Vlachopoulos, N., Walters, D.L., Burgess, P.G. and Allen, T.M. (2006) "The influence of facing rigidity on the performance of two geosynthetic reinforced soil retaining walls", *Canadian Geotechnical Journal*, v 43, n 12, p 1225-1237.
- Christopher, B.R., Leshchinsky, D. and Stulgis, R. (2005) "Geosynthetic-Reinforced Soil Walls and Slopes: US Perspective", *International Perspectives on Soil Reinforcement Applications*. ASCE Geotechnical Special Publication No. 141, ASCE Press, Reston, Virginia, January 2005, ISBN 0-7844-0769-X, 166 p.
- Elias, V., Christopher, B.R. and Berg, R.R. (2001) "Mechanically Stabilized Earth Walls and Reinforced Soil Slopes Design and Construction Guidelines", Report No. FHWA-NHI-00-043, *National Highway Institute, Federal Highway Administration*, Washington, D.C. March.
- Karpurapu, R.G. and Bathurst, R.J. (1995) "Behaviour of Geosynthetic Reinforced Soil Retaining Walls Using the Finite Element Method", *Computers and Geotechnics*, v 17 n 3, p 279-299.
- Lade, P.V. and Jakobsen, K.P. (2002) "Incrementalization of a Single Hardening Constitutive Model for Frictional Materials", *International Journal for Numerical and Analytical Methods in Geomechanics*, v 26, p 647-659.
- Lade, P.V. and Kim, M.K. (1995) "Single Hardening Constitutive Model for Soil, Rock and Concrete", *International Journal Solids and Structures*, vol. 32, n.14, pp. 1963-1978.
- Lade, P.V. and Kim, M.K. (1988) "Single Hardening Constitutive Model for Frictional Materials- II. Yield Criterion and Plastic Work Contours" *Computers and Geomechanics*, 6, pp. 13-29
- Lade, P.V. and Kim, M.K. (1988b) "Single Hardening Constitutive Model for Frictional Materials - III. Comparisons with Experimental Data." *Computers and Geomechanics*, 6, pp. 31-47.
- Kim, M.K. and Lade, P.V. (1988) "Single Hardening Constitutive Model for Frictional Materials- I. Plastic Potential Function" *Computers and Geomechanics*, 5, pp. 307-324.
- Yang, K.-H. (2009) "Stress Distribution within Geosynthetic-Reinforced Soil Structures", PhD Dissertation, Department of Civil Architectural and Environmental Engineering, the University of Texas, Austin.